A $N \times N$ Architecture for 2-D Mirror-Type Optical Switches

Shou-Heng Chen, Kuang-Chao Fan, Tien-Tung Chung, and Yao-Joe Joseph Yang, *Member, IEEE*

***Abstract*—This paper presents a switching architecture for any large port number optical cross connecting switch. We show the switching arrangement and the construction process to realize mirror-type optical switches. The proposed architecture refers to the Waksman network. Compared to other switching architectures, this architecture uses a minimum number of mirrors. Four guiding rules of the mirror arrangement method are proposed to assist building up a large port number mirror-type optical switch in an efficient way. By the analysis of all loss sources, the design parameters of the mirror are identified. The expandability and feasibility are verified. Furthermore, by an expert system, we can build up a lookup table to reduce the control complexity. The generalized simulation results show that the optical switch architecture of this paper is capable to archive the Bell Communications Research (BELLCORE) specification requirements for low and high port numbers.**

***Index Terms*—Insertion loss analysis, $N \times N$, network architecture, optical switch.**

I. Introduction

OPTICAL communication networks are built worldwide to provide high-speed and high-capacity transmission, utilizing the technology of dense wavelength-division multiplexing (DWDM). The optical switch plays an important role in fiber-optic communications for mapping wavelengths from the input ports to the proper output ports based on their destination. Hence, the popularization of optical switch is one of the keys for the future DWDM network development. The requirements for an optical switch include compactness, low power consumption, excellent optical performance, and low cost. The low port number switches (1×2, 1×4, and 2×2) have been developed since many years and are essential components in optical communication networks. Although piling up low port number switches to form a high port number optical switch is possible, such a solution, however, will proportionally increase the size, cost, system complexity, and insertion loss.

Manuscript received October 29, 2008; revised January 05, 2009 and February 19, 2009. First version published April 24, 2009; current version published July 22, 2009. This work was supported in part by the National Science Council under the project title of "Development of Micro/Nanotechnologies on the System and Components of Optical Switches" (Contract NSC 94-2212-E-002-058, NSC 94-2212-E-002-061). The support by the National Taiwan University Nanoelectromechanical System (NTU NEMS) Research Center for fabrication facility is greatly appreciated.

The authors are with the Department of Mechanical Engineering, National Taiwan University, Taipei 106, Taiwan (e-mail: d9452202@ntu.edu.tw; fan@ntu.edu.tw;; ttchung@ntu.edu.tw; yjy@mems.me.ntu.edu.tw).

Color versions of one or more of the figures in this paper are available online at http://ieeexplore.ieee.org.

Digital Object Identifier 10.1109/JLT.2009.2017280

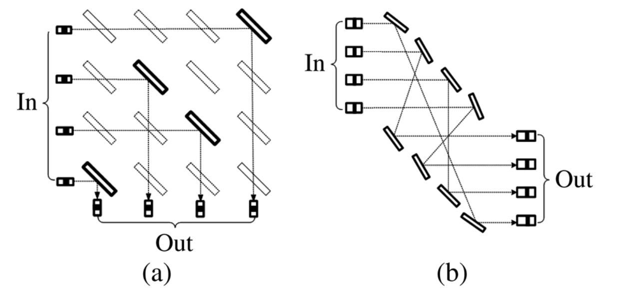

Fig. 1. Optical cross connections switch architectures. (a) 2-D architecture. (b) 3-D architecture.

The optical cross connect (OXC) is one kind of optical switch architectures that has been considered as the most promising candidate for the large port number application. It can be applied to microelectromechanical systems (MEMS) or mechanical optical switches by the reflection of mirrors to change the optical signals. This kind of optical switch has the advantages of low crosstalk, polarization-dependent loss, and wavelength dependency. For this reason, as of today, the OXCs optical switch plays an important role in the business market of the DWDM technology. The OXCs can be divided into two general switching architectures: the 2-D structure and the 3-D structure [1]. The traditional 2-D architecture uses N^2 mirrors to reflect N inputs to N outputs, as shown in Fig. 1(a). Each mirror needs only to provide two states (ON/OFF) for the light path at the cross position. This architecture has the advantages of simpler fabrication, easier controllability, and strictly nonblocking switching condition, but it needs a large number of mirrors and has the problem of different optical paths that will result in different optical losses. It inevitably requires a large physical size. The 3-D architecture uses $2N$ mirrors to reflect N inputs to N outputs, as shown in Fig. 1(b). There are two mirror arrays in the 3-D architecture. The first mirror array reflects all input light beams to the respective designated second mirror array, and the second mirror array reflects the light beams to the designated outputs. Through the two mirror arrays, the output light beams are parallel to the input light beams. In order to meet low power loss requirements, each mirror needs to be rotated precisely by a complicated servo control system to achieve an accurate position. This two-stage actuator control is very complicated.

In recent years, some researchers have proposed to improve the expansibility of the 2-D architecture. Yeow provided a new crossbar switching design methodology that reduced the number of the mirrors, improved the optical path difference, and reduced the distance of free-space propagation of the light beam [2]. Kuo and Yin combined the use of double-sided and

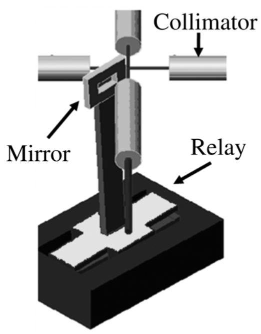

(a) (b)

Fig. 2. Principle of a double-sided mirror-type 2 × 2 optical switch. (a) Transmission state. (b) Reflection state.

single-sided mirrors according to the Clos network architecture that conforms to the optical permutation requirement [3]. The configuration of the mirrors also eliminates the problem of optical path differences. The Clos network constructed by 2 × 2 switch units is also called the Benes network. Ma and Kuo have proposed the Benes connecting principle to design different multistage optical switches [4], [5]. The Benes architecture can reduce the number of mirrors and improve the fabrication limit. Nevertheless, the input and output port number is only accepted to be a power of 2 and the number of mirrors is not the minimum.

In this paper, we apply the arbitrary Waksman network theory [6]–[8] to develop a 2-D $N \times N$ optical switch architecture. Through the arbitrary Waksman network, we can further enhance the advantage of the Benes network, for instance, reducing the number of mirrors, improving fabrication limit, and being applicable to an arbitrary number of input and output ports. The basic unit of this architecture is a 2 × 2 double-sided mirror-type optical switch developed by the authors' group, as shown in Fig. 2. The mirror is mounted on a metal arm, which is switched by a mechanical relay. In this paper, we developed four guiding rules to help to construction the mirrors architecture. Meanwhile, we present all the possible optical loss sources in the mirror-type optical switch. Finally, we can verify the practicability and feasibility of our architecture by the analysis and experimental results.

II. The Architecture of Arbitrary Port $N \times N$ Optical Switch

The matrix architecture of OXCs switches has the advantages of a binary control algorithm and a strict nonblocking switching condition, such that any input can be permutated to any output without influencing the established permutation states. However, as the port number is increased, there are disadvantages of the large number of the mirrors and optical path differences. This will limit the performance and the fabrication process of the optical switch. In this paper, we extend the use of a 2 × 2 optical switch as the basic unit and adopt the Waksman switching network theory to form the generalized architecture configuration.

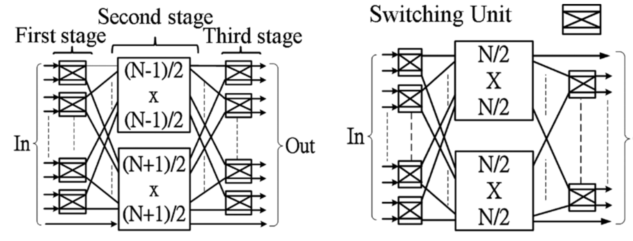

(a) (b)

Fig. 3. Waksman network construction. (a) Odd input type. (b) Even input type.

A. Switching Network Theory

According to the mathematical theory, the binary switching network needs at least $\log_2(N!)$ switching units to realize all permutation states of N input and N output ports [7]. The Benes network is constructed by binary switching units to form the switching network. It needs $N \times (\log_2 N) - N/2$ switching units to realize all permutation states. The number of switches for the Benes network is an obvious improvement in the development of high port number optical switches. However, the number of input ports must be a power of 2.

The Waksman network has the minimal number of switching units, which is less than the Benes network. In each step of the recursive expansion, the Waksman network spares one switching unit compared to the Benes network to construct its network. Further works by Beauquier and Darrot[8] have shown that an arbitrary size Waksman network allows an arbitrary input and output counts. In this paper, we refer to the arbitrary size of Waksman network and use two kinds of mirrors to realize the switching architecture. First, the moveable mirrors are the switching units of the arbitrary size Waksman network. Second, the fixed mirrors are to restrict the signal route and conform to the network theory.

B. The Guiding Rules of Mirrors Arrangement

The construction process of an arbitrary size Waksman network architecture [8] uses the top-down method to arrange all switching units, as shown in Fig. 3. At first, the numbers of switching units in first stage and third stage have to conform to the requirement of input and output numbers. Next, the second stage can be seen as a new three stages network architecture. The key point of the process is to break down the second stage of the Waksman network until only a 2 × 2 switching unit is left in the second stage. After the top-down process, we refer to the network architecture and start the bottom-up process to arrange the position of the mirrors. At first, we build up the minimal second stage in network architecture. Next, we build up the first stage and the third stage to accomplish a three stage. In the button-up process, the smaller three stage architecture can be the second stage of the larger three stage architecture. Four guiding rules are used to help arrange the mirrors as follows:

1) We draw the architecture and signal path by the arbitrary size Waksman network theory. After the top-down process, we start the bottom-up process from the two basic switching architectures, the 3 × 3 and the 4 × 4 switches, as shown in Fig. 4.

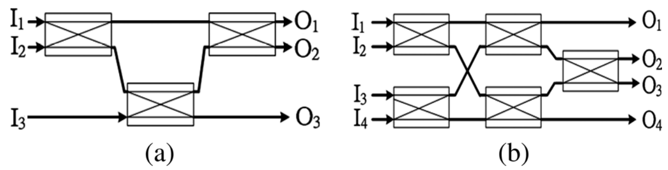

Fig. 4. Arbitrary size Waksman networks architectures. (a) 3 × 3 Switch. (b) 4 × 4 Switch.

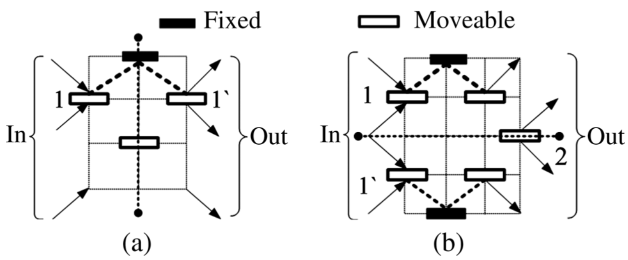

Fig. 5. Mirror arrangements of the two basic architectures. (a) 3 × 3 Switch. (b) 4 × 4 Switch.

2) The large port number optical switch is constructed recursively from the two basic switching architectures. Unlike the arbitrary size Waksman network architecture using a 1 × 1 switch and a 2 × 2 switch, we use a 3 × 3 switch and a 4 × 4 switch to be the basic switching architectures; those are shown in Fig. 5. This is because neither a 1 × 1 nor a 2 × 2 switch network is a three-stage structure. In the second stage of Fig. 5(a), the 1 × 1 switching unit is a straight channel that does not need any mirror. The 2 × 2 switching unit only needs one mirror to permute the optical signal. Therefore, both the 3 × 3 switch and the 4 × 4 switch are the basic odd and even architectures in our study.
3) Comparing Figs. 4 and 5, the position of the switching unit in Fig. 4 and the moveable mirror in Fig. 5 are in correspondence. In the construction process, the fixed mirrors are used to restrict the optical path routes to conform to the network architecture requirement in Fig. 4. The method to find the positions of fixed mirrors as follow: At first, we set all moveable mirrors in reflection state. Next, we trace all optical signals from input ports to output ports. Each input should have a corresponding output port. If the input signal is divergent, we will trace back the signal from nonmatch output ports. One input signal and one output signal will cross at a point, as shown in Fig. 5. The cross points are the positions of fixed mirrors.
4) Using the symmetrical character of the architecture, we can speed up the mirror arrangement process of first and third stage. The odd architecture is symmetrical to the vertical center line, as shown in Fig. 5(a). After the arrangement of the second stage, we need to only arrange the input side of the mirrors 1–3 in Fig. 6(a) and then fold these mirrors along the vertical center line to the other side to accomplish the mirrors 1′, 2′ and 3′. Likewise, the even architecture is symmetrical to the horizontal center line, as shown in Fig. 6(b). We need to arrange only half of the mirrors 1–4 and then fold these mirrors to accomplish the mirrors 1′, 2′ and 3′.

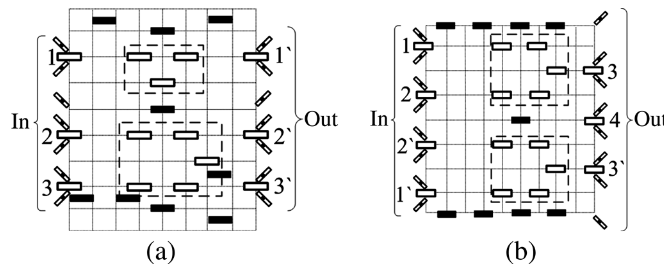

Fig. 6. Examples of two optical switches. (a) 7 × 7 Switch. (b) 8 × 8 Switch.

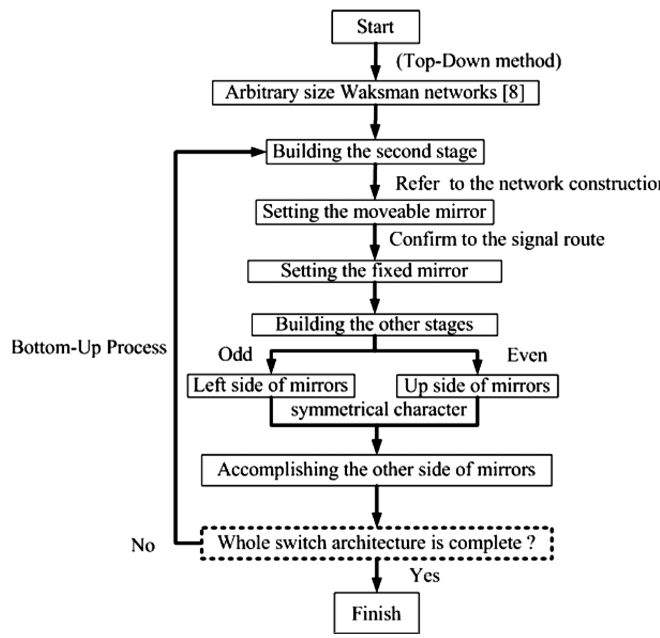

Fig. 7. Flow chart of the mirror arrangement.

The flow chart of the mirror arrangement process is shown in Fig. 7. The four guiding rules mentioned above assist the process to arrange the mirrors. More examples are shown in Fig. 6. Fig. 6(a) is a 7 × 7 switch architecture that comprises one 3 × 3 basic switching architecture and one 4 × 4 basic switching architecture arranged in the second stage. Fig. 6(b) is a 8 × 8 switch architecture that comprises two 4 × 4 basic switching architectures in the second stage. Following the flow chart and guiding rules presented in this paper, we can successfully and rapidly arrange arbitrary port number optical switches.

III. The Comparison of Switching Architectures

In the switching process of a traditional matrix structure, each optical path needs only one reflection by a mirror to connect to the designated output, but it needs a lot of mirrors to accomplish all the required permutations. Although a multistage switching network can reduce the number of switching unit, most of the optical paths need more than one reflection. The number of reflections and the mirror quality are the key points in 2-D architecture optical switches, because the more reflections, the higher the power loss. Hence, prior to the design of an optical switch, we need to take care of the character of the multistage switching in our study, as follows:

1) *The number of mirrors:* According to the theory of the Waksman network, the number of switching units for the worst-case is shown in (1), where $\lambda = -\log_2 \times(\log_2 e)$ and N is the number of input ports.

$$U(N) = N\log_2 N - N(2^{\lambda} - \alpha) + 1. \quad (1)$$

However, when the number of input ports is a power of 2, the number of switching units is $N \times (\log_2 N - N + 1)$. In order to simplify the analysis process, we use a power of 2 for the input number to analyze the feasibility in our study. We use two kinds of mirrors, moveable mirrors and fixed mirrors, to build up all optical channels. The number of the moveable mirrors is the same as the number of the switching units in the Waksman networks. The number of the fixed mirrors is $(N/2-1)\times\log_2 N$ in our architecture. The comparison of the mirror numbers is shown in Table I. The first column is the minimum number of the switching network, which is constructed by 2 × 2 binary switches. The N input and N output network has N! possible permutation states. Therefore, it needs at least $\lceil \log_2 N! \rceil$ binary switches in the network [7]. The second column is the number for the traditional matrix architecture, which increases the mirror number dramatically as the port number increases. The numbers of moveable mirrors and fixed mirrors are divided by a slash in the third and fourth column. The third column is the number for Ma and Kuo's architecture [4] with the Benes network. The fourth column is the mirror number for our proposed architecture with the Waksman network. Table I shows that the higher the input port number, the bigger the difference in the number of mirrors between our architecture and the matrix architecture. In all networks, the number of mirrors for our proposed architecture is the most close to the theoretical value. It can also clearly be seen that our proposed architecture needs a smaller number of mirrors than the Ma and Kuo's architecture.

2) *The optical path length:* In the design process of large port number optical switches, we need to take care of the optical path length in the proper range to meet the fabricating limitations [9]. Furthermore, a good switch architecture should minimize the propagation distance between the input and output ports [2]. In our architecture, we assume that the minimal length between two moveable mirrors is t. That is the diagonal length of the unit block, as shown in Fig. 7. The optical path length between any input to any output can be expressed by

$$L(N,t) = [2(N - \log_2 N) - 1] \times t. \quad (2)$$

According to the research that has been proposed [4], the Benes network architecture can shorten the optical path by about 40% compared to the traditional matrix architecture. In our study, the distance between the second stage and the third stage is even shorter than for the Benes networks architecture, as shown in Figs. 1(c) and 7(b). Given $N = 8$ and $N = 16$, the path lengths for the Benes architecture are 12t and 28t, respectively. In our study, the path lengths are 9t and 23t, respectively. The difference of the path length is $(2n - 1) \times t$, where $n = (\log_2 N) - 1$.

TABLE I
COMPARISON OF THE NUMBER OF MIRRORS

Method / Ports	Least Bound	Matrix	Ma and Kuo	Proposed
4	5	16	6/4	5/2
8	16	64	20/14	17/9
16	45	256	56/38	49/28
32	118	1024	144/94	129/75
64	296	4096	352/222	321/186

3) *The number of reflections:* In the multistage switching architecture, the stage number increases with the port number; it is $(2\log_2 N) - 1$. All optical paths have to pass all stages in order to arrive at their designated outputs. According to the different switching requirements, the number of reflections of each mirror is different. In the Benes architecture, the maximum number of reflection is $4(\log_2 N - 1) + 1$, and the minimum number is zero. In our architecture, the maximum number of reflection is $4(\log_2 N - 1) - 1$, and the minimum number is zero. The maximum number difference of two architectures is 2. However, the difference of average reflections number will increase with the increase of port number, which results in the increase of the mirror.

4) *The complexity of control method:* The multistage architecture can successfully reduce the number of switches, but there is a tradeoff between the number switches and the complexity of the control method. The N port switching network needs N! permutation states. In the matrix architecture, one switching unit is responsible for one specified optical path and all optical paths are independent. In other words, each permutation state has only one specific switching state of the mirrors. However, the switching unit in a multistate architecture is a binary switching mechanism; the result is that the optical paths are dependent. In our study, M switching units have 2^M permutation states. When the port number is greater than 2, the number of switching states is greater than the number of permutation states. Hence, each permutation state may have more than one switching state of the mirrors, and the greater the number of mirrors the more complex the mirror control method. Therefore, the control method of the Benes network is more complex than that of the Waksman network.

IV. The Analysis of All Power Loss Sources

In this section, we try to analyze all possible loss sources for the estimation of the performance in the next section. The losses of mirror type 2-D optical switches come from three factors, namely, the optical transmission, the mirror alignment, and the mirror reflection. The optical transmission loss is a dominant factor in free-space-based optical switches. When the light is emitted from the fiber, the Gaussian beam diverges and the loss increases significantly. In order to overcome the beam divergence, there are designs using a lens in front of the fiber [10]–[15]. This can extend the optical path length and ensure the

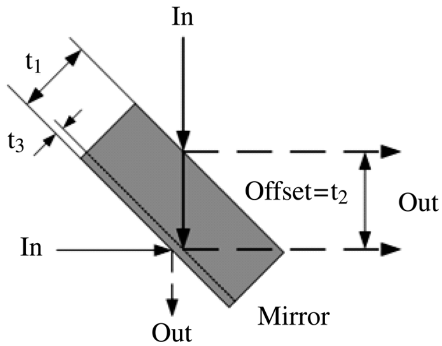

Fig. 8. Offset misalignment by the mirror thickness.

efficiency of the power coupling, but it also has the drawback of higher costs. The combination of the fiber with the lens is called a collimator, which can easily be purchased from the market and has the coupling loss being lower than 0.2 dB. Hence, in this section, we will discuss the other influences in our architecture.

A. The Loss by an Optical Misalignment

The alignment is the key to the optical switch performance. In our study, we use collimators at input and output fiber heads. The analysis of the collimator misalignment has widely been discussed [16]. There are three types of misalignments causing the coupling losses, which are the offset misalignment, the angular tilt misalignment, and the separation misalignment. The coupling efficiency could use the Gaussian field approximation method to characterize each misalignment simultaneously [17]. The details of each loss are explained as follow:

1) *The offset misalignment*: The mirror-type optical switch is influenced by the thickness of the mirror (t_1), which causes an inevitable offset and misalignment (t_2), where $t_2 = \sqrt{2}t_1$, as shown in Fig. 8. This increases the insertion losses of the output channels during the reflection state. The general formula of the offset loss is derived, as shown in (3), based on the analysis in [17]. η_1 is the offset misalignment insertion loss, λ is the wavelength of the light, *w* is the beam waist, *n* is the refractive index, *z* is the working distance between a pair of collimators, and *t* is the offset distance.

$$\begin{aligned}\eta_1 &= 10\log(P_{\text{loss}}/P_{\text{total}})\\ &= 20\times n^2\pi^2(2w^2)\times t_2^2\\ &\quad /[\ln 10\times\lambda^2\times Z^2+\pi^2 n^2 4w^4]. \qquad (3)\end{aligned}$$

The calculation and experimental results of the lateral offset of the collimator are shown in Fig. 9 $(\lambda = 1550\ \text{nm}, w = 0.5\ \text{mm}, n = 1\ \text{and}, z = 50\ \text{mm})$. It shows that the collimator has a superior feature with respect to the lateral offset. In the design process, we take the parameter of the mirror thickness into account.

2) *The angular tilt misalignment:* The collimator is sensitive to the angular tilt misalignment, and the parallelism of the mirrors affects the performance of 2-D optical switches. When the mirror has an angular error of θ, this results in 2θ of angular misalignment of the beam and in $R\times\tan 2\theta$ of the lateral offset, as shown in Fig. 10, where *R* is the distance between the mirror and the receiving port. The lateral offset resulted from the angular tilt misalignment increases the optical path length. The general formula of the angular misalignment loss is derived in (4), where η_2 is the angular tilt misalignment insertion loss, λ is the wavelength of the light, *w* is the beam waist, *n* is the refractive index, *z* is the working distance between a pair of collimator, and θ is the misalignment angle.

$$\begin{aligned}\eta_2 = &\ 20\times(n\pi w/\lambda)^2\\ &\times\left[(nZ/n\pi w^2)^2+2\right]\sin^2\theta\\ &/\left\{\ln 10\times\left[(nZ/n\pi w^2)^2+4\right]\right\}. \qquad (4)\end{aligned}$$

Fig. 11 shows the comparison of the experimental and calculated results with angular misalignment $(\lambda = 1550\ \text{nm}, w = 0.5\ \text{mm}, n = 1\ \text{and}, z = 0\ \text{mm})$. In the design process, we take the parallelism of all mirrors into account.

3) *The separation misalignment:* In the free-space-based optical switch, the single-mode or multimode pigtailed fiber collimator have widely been used. This is because the collimator could provide a large separation distance between

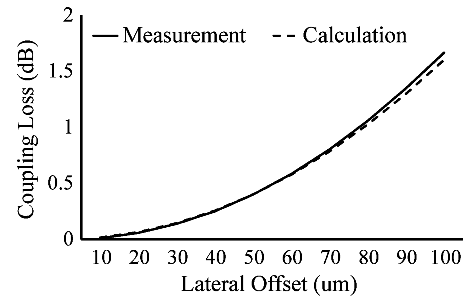

Fig. 9. Calculated and experimental results of the lateral offset.

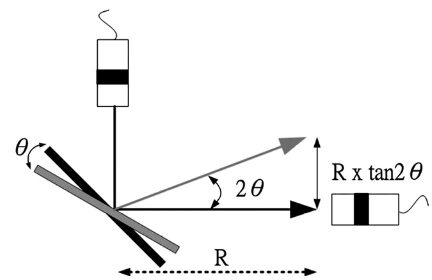

Fig.10. Angular misalignment caused by the mirror rotation.

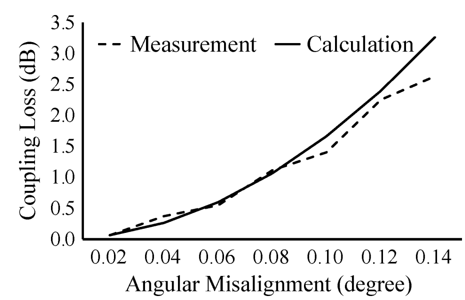

Fig. 11. Calculated and experimental results due to angular misalignment.

the input and the output ports. For getting the best collimator coupling efficiency in the assembly process, the collimator must be separated by a proper distance. The separation misalignment is a serious problem in the traditional matrix structure because of the optical path difference in each permutation state, as shown in Fig. 1(a). Thus, there were studies to design a new configuration or to use an optical component to eliminate the optical path difference [18], [19]. In our architecture, we need only to take the switching architecture size into account and place the collimators at suitable working distance. The separation misalignment can be neglected by putting the input collimator and the corresponding output collimator parallel to each other, as shown in Fig. 7.

B. The Loss Caused by the Mirror Reflection

The reflection efficiency of the mirror determines the performance of a mirror-type optical switch. In our architecture, the light has a maximum number of reflections of $4(\log_2 N - 1) - 1$. Hence, the loss caused by the mirror reflection will become a major topic of the power performance in a high port number optical switch. In this paper, we must analyze all possible loss sources resulting from the mirrors. It could be determined by the following four factors, which are the surface reflectivity, the surface roughness, the proportion of the mirror diameter to the light beam diameter, and the mirror curvature. The details are described as follows:

1) *The surface reflectivity:* In order to have a high reflectivity of the mirror, it has to be coated with a high reflectivity material. Gold-coated and the aluminum-coated mirrors are popular types of mirrors and reach a maximum reflectivity of 97.5% and 97% at a film thickness of 60 and 40 nm, respectively [20]. Thus, these two materials are usually selected to coat the silicon to be the surface material of a highly reflecting mirror.
2) *The surface roughness:* The mirror surface roughness causes unavoidable losses that result from optical scattering. For a gently sloped surface with a Gaussian light distribution, the loss caused by scattered light can be estimated by (5) [21], where α is the surface roughness, φ is the incidence angle, and λ is the wavelength of the light. The roughness is in the exponential term. Therefore, we must determine a suitable mirror fabrication process and confirm that the roughness is satisfying the requirements in the design process.

$$p_{\text{loss}}/p_{\text{total}} = 1 - \exp\left[-(4\pi\alpha\cos\varphi/\lambda)^2\right]. \tag{5}$$

3) *The proportion of the mirror diameter to the beam spot size:* The collimator could provide a large optical path length. However, this yields a large beam spot size in the transmission process. The beam spot size of the collimator is larger than the single-mode or multimode fiber. Therefore, we should take care that the diameter of the mirror is large enough to reflect the total light power. The loss can be estimated by (6), where *r* is the mirror diameter and *w*(*Z*) is the beam spot size at distance *Z* from the outlet of the collimator. When the mirror diameter is $\sqrt{2}$ times the beam spot size, the loss is about 0.08 dB.

$$p_{\text{loss}}/p_{\text{total}} = \exp\left[-2r^2/w(Z)^2\right] \tag{6}$$

4) *Mirror curvature:* In all the above-mentioned losses, we assume that the mirror is flat. However, the curvature of the mirror will change the fiber coupling mode and the beam spot size and will thus decrease the coupling efficiency. The fiber coupling efficiency is given in (7), where $E_f(x,y)$ is the function of the fiber complex amplitude, $E_w(x,y)$ is the function of the beam coupling into the fiber, and Ex' is the complex conjugate of Ex.

$$E = \left|\iint E_f(x,y)E'_w(x,y)\partial x\partial y\right|^2 \Big/ \left[\iint E_f(x,y)E'_f(x,y)\partial x\partial y\cdot\iint E_w(x,y)E'_w(x,y)\partial x\partial y\right]. \tag{7}$$

TABLE II
SIMULATION CONFIGURATION AND PARAMETER

Type	Parameter
Wavelength	1550 nm
Fiber	SMF-28e
Working Distance	50 mm
Beam Waist	500 µm
Lens	C-Lens
Coating	AR
Coupling Loss	-0.2dB
Simulation	POP
Optimization	POPD

The fiber coupling efficiency *E* is defined as an overlap integral between the fiber $E_f(x,y)$ and the beam $E_w(x,y)$. In our study, we use the commercial software ZEMAX to calculate the coupling efficiency and to simulate the curved mirror situation. The simulation condition and parameters are listed in Table II. The parameters of the collimator are taken from the data sheets of market products. ZEMAX have several calculation tools for different simulation circumstances. In our study, the propagation of light between two collimators is a coherent process and each step of the wavefront coherently interferes with the other step. Physical optics propagation (POP) is an appropriate method to calculate the beam through the optical system surface by surface in ZEMAX. Before the simulation, we have to define each parameter of the surface, such as air, fiber, lens, and fiber. In the simulation process, we use the optimization tool of ZEMAX, POPD merit function, to optimize the distance between the fiber and the lens in the collimator. The actual coupling loss of collimator is our target of optimization. After we approach the target, we change the position of the mirror and the radius of curvature and then repeat the simulation process. The curved mirror is located at three different positions between the input and output fibers, as shown in Fig. 12. The total distance is 50 mm, the first position of the mirror in front of the input fiber is 5 mm, the second position is in the middle of the total distance, and the third position is at 5 mm before the output fiber. The result of the

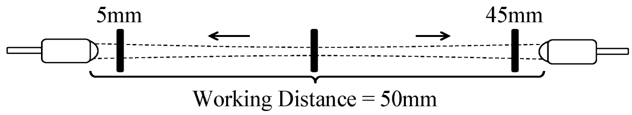

Fig. 12. Three positions of the mirror between the collimators.

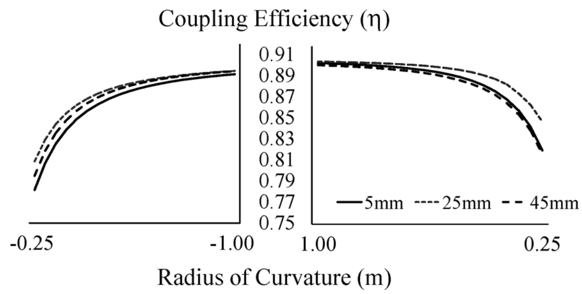

Fig. 13. Coupling efficiency at three positions with different curvature radius.

TABLE III
DESIGN PARAMETERS OF THE MIRROR

Loss Source	Mirror	Parameter	Value
Collimator lateral Misalignment	Thickness	t_2 (3)	1.8 um
Surface Scattered	Roughness	A (5)	5.7 nm
Mirror Size	Area	r (6)	4 mm^2
Mirror Curvature	Curvature	c	0.5 m
Surface Material	Material	Au、Al	Au/Cr

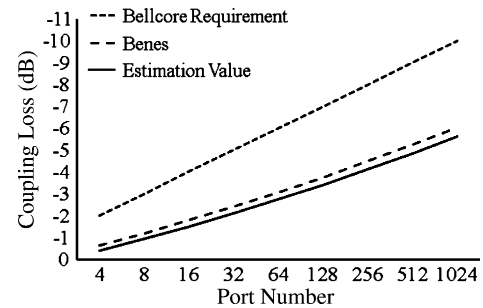

Fig. 14. Estimation of the coupling loss in this work.

simulation is shown in the Fig. 13. The coupling efficiency reduces dramatically when the curvature radius is within ± 0.5 m. A concave and convex mirror in the simulation result has the same effect on the coupling efficiency. The mirror position in the middle has the maximum coupling efficiency, because the wavefront of the beam is flat and the focus point has a minimum spot size. Hence, the mirror in the middle has less effect than at others positions. It is also noticed that the effect of different mirror positions is insignificant.

V. PERFORMANCE ANALYSES

A. The Power Loss Estimation

After the analyses of all loss sources, we need to synthesize and estimate the performance in order to verify the expandability and feasibility of the proposed arbitrary size $N \times N$ optical switch architecture. The power loss estimation can be divided into two main parts, which are the assembly loss and reflection loss. The assembly loss is independent of the number of reflections. In other words, it does not increase with the port number. Besides, the optical alignment will depend on the precision of the alignment stage and the alignment method. Therefore, in this paper, we ignore the assembly loss in the loss estimation process. The calculation of the reflection loss combines all losses resulting from the mirror and the maximum reflection number of the mirrors. The design parameters of the mirror are listed in Table III. The authors' group has developed a thin-film mirror that is fabricated by a simple MEMs process. The mirror is coated by an ultrathin high reflective Au/Cr film on both sides (the thickness is less than 1.8 μm, the reflection area is 2 mm $\times$ 2 mm, the surface roughness is 5.7 nm, and the curvature radius is larger than 0.5 m) in order to allow a double-sided reflection. We use this parameters of the mirror in the estimation of the power loss. The loss of the first three rows in Table III can be calculated by (3), (5), and (6). The curvature radius is big enough that the curvature-induced error can be ignored. Fig. 14 illustrates the comparison of the estimation of the power loss and the Bell Communications Research (BELLCORE) [22] requirement for low and high port numbers. The value of coupling loss is the addition of each estimated loss factor. The estimation losses of port number in our architecture are all less than BELLCORE requirements. Moreover, the trend in our architecture is almost straight, and the slope is less than the BELLCORE requirement, which means the higher port number, the lower the power loss. The result of the loss estimation ignores the assembly loss. The assembly loss is a constant value that is independent of the port number. In each case, we allow for the possible assembly loss. Hence, the analysis results verify the expandability and feasibility of the arbitrary size multistage $N \times N$ optical switch architecture in our study.

B. The Optimization Method of Optical Path Selection

The Waksman network can provide the advantage to reduce the number of mirrors. However, it yields that one permutation state may have more than one switching state of the mirrors. We need to select *N*! permutation states with $2^{S(N)}$ mirror switch states, where *S*(*N*) is the total number of the mirrors and *N* is the port number. It increases the complexity of the switching rule. In our study, we use an expert system to select *N*! permutation states in $2^{S(N)}$ mirror switching states. The result of this selection needs to match *N*! permutation states of the $N \times N$ switch system, keeps the minimum loss in redundant permutation statuses and conforms to the output loss differences of BELLCORE requirement. The difference in the power loss of all output channels can be expressed by (8) [22], where i is the input port, and j and k are the output ports.

$$\Delta P_{\text{loss}} = \max |10 \log(t_{ji}/t_{ki})| \leq 0.5 \log_2 N. \qquad (8)$$

The expert system is a knowledge-based analysis method. Prolog has been used to program the expert system used in our study. The programming in our study has four parts. First, we build up the optical path routes and the multilayer architecture, as shown in Fig. 15. When optical input passes through each layer to optical output, we can record the trace of the optical

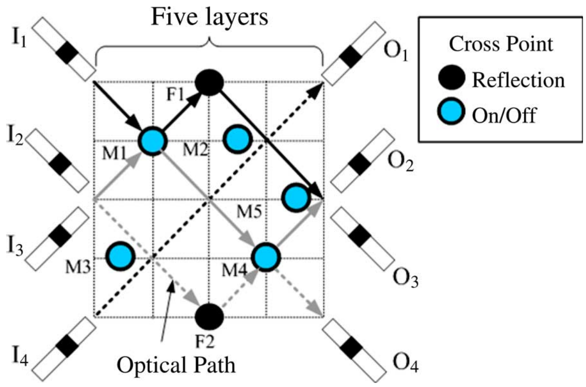

Fig. 15. Depiction of one optical path selection of a 4 × 4 optical switch.

path. Second, we describe the situation of the optical paths at each cross point. The optical path in the node has only two possible paths to the next layer, pass or reflection. Third, we need to define all components in the architecture. The reflection nodes are *F*, the ON/OFF nodes are *M*, the optical inputs are *I*, and optical outputs are *O*. Fig. 15 illustrates one example of the permutation states. The input signal I_1 is reflected by the mirror M_1 and the mirror F_1 into the output O_3. Similarly, all the optical paths can be derived, and we can verify whether all the permutation states have been archived. Finally, we set the score to all optical paths. Appling the loss value to each node, we can record the total losses of the optical path. According to the expert system in our study, we not only can conform to the requirement of output loss differences but also rule out the redundant permutation states. Therefore, we can build up a lookup table in order to reduce the control complexity.

VI. Conclusion

The architecture of arbitrary size multistage $N \times N$ optical switches has been developed in this paper. By adopting the arbitrary Waksman network, we need a minimum number of switching mechanisms compared to other 2-D switching architectures. The presented architecture is better than the Benes architecture in terms of four indicators, namely, the number of mirrors, the optical path length, the number of reflections, and the complexity of control method. To realize the mirror arrangement, we have developed four guiding rules to help to arrange the mirrors. We have also theoretically analyzed and measured all the loss sources to verify the expandability and the feasibility of this architecture. The results show that it can conform to the coupling loss requirements for a low port number as well as a high port number. By an expert system, we can rule out the redundant permutation states and build up a lookup table in order to reduce the control complexity. This architecture can develop not only mirror-type optical switches but also any optical switch that uses binary switches as basic switching unit.

References

[1] A. Q. Liu, X. M. Zhang, V. M. Murukeshan, Q. X. Zhang, Q. B. Zou, and S. Uppili, "An optical cross connect (OXC) using drawbridge micromirrors," *Sens. Actuat. Phys.* 2002, pp. 227–238.

[2] J. T. W. Yeow and S. S. Abdallah, "Novel MEMS L-switching matrix optical cross-connect architecture: Design and analysis—Optimal and staircase-switching algorithms," *J. Lightw. Technol.*, vol. 23, no. 10, pp. 2877–2892, Oct. 2005.

[3] G. S. Kuo and Y. Yin, "Integrated multistage MEMS-based optical switch," in *Proc. Symp. Des. Test, Integr. Packag. MEMS/MOEMS*, 2003, pp. 113–116, IEEE Computer Society.

[4] X. Ma and G.-S. Kuo, "A novel integrated multistage optical MEMS-mirror switch architecture design with shuffle Benes inter-stage connecting principle," *Opt. Commun.*, vol. 242, pp. 179–189, 2004.

[5] X. Ma and G. S. Kuo, "A novel 2D MEMS-based optical cross connect with greatly reduced complexity," *Proc. SPIE—Int. Soc. Opt. Eng.*, pp. 463–472, 2004.

[6] L. J. Goldstein and S. W. Leibholz, "On the synthesis of signal switching networks with transient blocking," *IEEE Trans. Electron. Comput.*, vol. EC-16, no. 5, pp. 637–641, Oct. 1967.

[7] A. Waksman, "A permutation network," *J. ACM*, vol. 15, pp. 159–163, 1968.

[8] B. Beauquier and E. Darrot, "On arbitrary size Waksman networks and their vulnerability," *Parallel Process. Lett.*, vol. 12, pp. 287–296, 2002.

[9] R. R. A. Syms, "Scaling laws for MEMS mirror-rotation optical cross connect switches," *J. Lightw. Technol.*, vol. 20, no. 7, pp. 1084–1094, Jul. 2002.

[10] L. Zhao, J. Liang, W. Dong, A. Ming, W. Lan, X. Jin, W. Zhu, W. Wang, Z. Le, W. Chen, and L. Wang, "The packaging technology of optical switch arrays," *in Proc. SPIE.* Changchun, China, 2006, p. 60320.

[11] X. C. Shan, T. Ikehara, Y. Murakoshi, and R. Maeda, "Applications of micro hot embossing for optical switch formation," *Sens. Actuators Phys.*, vol. 119, pp. 433–440, 2005.

[12] L. Y. Lin, E. L. Goldstein, and R. W. Tkach, "On the expandability of free-space micromachined optical cross connects," *J. Lightw. Technol.*, vol. 18, no. 4, pp. 482–489, Apr. 2000.

[13] D.-M. Sun, W. Dong, G. D. Wang, C. X. Liu, X. Yan, B. K. Xu, and W.-Y. Chen, "Study of a 2 × 2 MOEMS optical switch with electrostatic actuating," *Sens. Actuators Phys.*, vol. 120, pp. 249–256, 2005.

[14] J. Bao, Z. Cao, Y. Yuan, and X. Wu, "A non-silicon micro-machining based scalable fiber optic switch," *Sens. Actuators Phys.*, vol. 116, pp. 209–214, 2004.

[15] D. T. Neilson, R. Frahm, P. Kolodner, C. A. Bolle, R. Ryf, J. Kim, A. R. Papazian, C. J. Nuzman, A. Gasparyan, N. R. Basavanhally, V. A. Aksyuk, and J. V. Gates, "256 × 256 port optical cross-connect subsystem," *J. Lightw. Technol.*, vol. 22, no. 6, pp. 1499–1509, Jun. 2004.

[16] C. S. Hsieh, C. Y. Wang, C. F. Song, and W. H. Cheng, "The coupling-loss characterization of an add/drop filter module in dwdm applications," *in Proc. 51st Electron. Compon. Technol. Conf.*. Orlando, FL, 2001, pp. 1431–1433.

[17] S. Yuan and N. A. Riza, "General formula for coupling-loss characterization of single-mode fiber collimators by use of gradient-index rod lenses," *Appl. Opt.*, vol. 38, pp. 3214–3222, 1999.

[18] T. W. Yeow, K. L. E. Law, and A. A. Goldenberg, "Micromachined L-switching matrix," in *Proc. IEEE Int. Conf. Commun.*, 2002, pp. 2848–2854. New York.

[19] T. W. Yeow, K. L. E. Law, and A. A. Goldenberg, "SOI-based 2-D MEMS L-switching matrix for optical networking," *IEEE J.Sel. Topics Quantum Electron.*, vol. 9, no. 2, pp. 603–613, Mar./Apr. 2003.

[20] M. Cao, Q. Hu, Z. Wan, and F. Luo, "A novel routing optical matrix swtiching method," *Opt. Commun.*, vol. 204, pp. 163–170, 2002.

[21] C. Marxer, C. Thio, M. A. Gretillat, N. F. de Rooij, R. Battig, O. Anthamatten, B. Valk, and P. Vogel, "Vertical mirrors fabricated by deep reactive ion etching for fiber-optic switching applications," *J. Microelectromech. Syst.*, vol. 6, pp. 277–285, 1997.

[22] Bellcore Technical Reference TR-NWT-001073, *Generic Requirements for Fiber Optic Switches* no. 1, 1994.

Shou-Heng Chen received the B.S. degree in the mechanical engineering from Chung-Yuan Christian University, Jhongli, Taiwan, in 2002, and the M.S. degree in mechanical engineering from the National Central University, Jhongli, Taiwan, in 2005, and he is currently working toward the Ph.D. degree at the National Taiwan University, Taipei, Taiwan, where he is currently engaged in research on optical switch, micro/nanomanufacture technology, and image processing.

Kuang-Chao Fan was born in Taiwan, on January 4, 1950. He received the B.Sc. degree from the National Taiwan University (NTU), Taipei, Taiwan, in 1972, the M.Sc. degree from The State University of New York, Buffalo, in 1976, and the Ph.D. degree from the University of Manchester Institute of Science and Technology, Manchester, England, in 1984, all in mechanical engineering.

Since August 1989, he has been a Professor of Mechanical Engineering at NTU, where he has promoted to the Distinguished and Chair Professor in 2007. He is the author or coauthor of around 100 journal papers and 200 conference papers published. His current research interests include manufacturing metrology, precision machining, optical switches and machine tool technology.

Prof. Fan is the Fellow of Society of Manufacturing Engineers (SME). In 2003, he received the Distinguished Research Award from the National Science Council, Taipei, Taiwan.

Tien-Tung Chung was born in Taoyuan, Taiwan, on September 16, 1953. He received the Bachelor's degree from the Department of Power Mechanical Engineering, National Tsing Hua University, Hsinchu, Taiwan, in 1976, and the Master's and Ph.D. degrees from the Department of Mechanical Engineering, National Taiwan University, Taipei, Taiwan, in 1980 and 1986, respectively.

Since August 1987, he has been with the Department of Mechanical Engineering, National Taiwan University, as an Associate Professor. He was also involved in military service for two years. His current research interests include structural optimization, computer-aided design, expert system, and reverse engineering.

Yao-Joe Joseph Yang (M'01) received the B.S. degree from the National Taiwan University, Taipei, Taiwan, in 1990, and the M.S. and Ph.D. degrees in electrical engineering from the Massachusetts Institute of Technology, Cambridge, in 1997 and 1999, respectively.

From 1999 to 2000, he was with the Coventor Inc., Cambridge, as a Senior Engineer. Since 2000, he has been with the Department of Mechanical Engineering, National Taiwan University (NTU), where he is currently an Associate Professor. He is also the Director of Computer-Aided Design (CAD) Technology, Center of Nanoelectromechanical Systems, NTU. His current research interests include microelectromechanical systems and nanotechnology.